Research Article

Journal of Labelled Compounds and Radiopharmaceuticals

Received 5 March 2008, Revised 20 October 2008, Accepted 20 October 2008 Published online 3 December 2008 in Wiley Interscience

(www.interscience.wiley.com) DOI: 10.1002/jlcr.1567

Dissociation kinetics determination of yttrium(III)-polyaminocarboxylates using free-ion selective radiotracer extraction (FISRE)

Denis Jurkin,[a]* Franz Josef Gildehaus,[b] and Birgit Wierczinski[c]

Free-ion selective radiotracer extraction (FISRE) is a technique combining ion exchange and the use of radiotracers in order to determine labilities of metal complexes. The aminocarboxylate chelates ^{90}Y-EDTA, ^{90}Y-DTPA as well as ^{90}Y-DOTATOC, a radiopharmaceutical for neuroendocrine tumor treatment have been studied by FISRE using Chelex cation exchanger within the pH range 5.0–7.4. Time-dependent speciation and dissociation rate constants have been determined in a time frame of 0.6 s–648 h. As indicated by thermodynamic constants, the lability decreases significantly with higher ligand denticity, cyclic coordination and upon peptide coupling resulting in the lability order Y-EDTA > Y-DTPA > Y-DOTA > Y-DOTATOC. Besides, studies of the effects of the metal/ligand ratio on FISRE suggest that – in contrast to EDTA and DTPA – cyclic ligands DOTA and DOTATOC tend to shield the ion exchanger from free yttrium ions after complex dissociation even at slight excess of metal ions.

Keywords: kinetic stability; yttrium-90

Introduction

Target-specific metalloradiopharmaceuticals are extraordinary important tools for diagnostic and therapeutic applications in current nuclear medicine. These molecules usually consist of a metallic radionuclide, a high-affinity targeting biomolecule (BM) attached to a metabolizable linker, as well as a bifunctional chelator (BFC) binding radioactive metal and the linker.[1–4] Ideally, the radiopharmaceutical delivers cytotoxic doses of radiation and/or a diagnostic marker specifically to the disease site. Nevertheless, following administration, the transport of the radionuclide to the target tissue may be reduced by e.g. clearance *via* liver and kidneys, metabolism, extrinsic protein binding, metal/chelate competition reactions (e.g. with Fe^{3+} or transferrin) or, particularly, dissociation of the metal-BFC complex releasing the free radioactive metal ion. Hence, in addition to biological affinity and pharmacokinetic behavior, the thermodynamic and kinetic stability of the metal-BFC complex at physiological pH is a crucial criterion for the applicability of a radiopharmaceutical.

Owing to remarkably high thermodynamic equilibrium constants *K*, polyaminocarboxylates as e.g. EDTA (ethylenediaminetetraacetic acid), DTPA (diethylenetriaminepentaacetic acid) and DOTA (1,4,7,10-tetraazacyclododecane-1,4,7,10-tetraacetic acid) are of particular interest as BFCs for ^{90}Y and lanthanide radiopharmaceuticals (Figure 1).[5–9] The inertness of the metal complexes – a feature that cannot be derived by thermodynamic data – was shown to be decisive for their *in vivo* release of free radioactive metal ions. For instance, in contrast to its ^{111}In-analogue, ^{90}Y-DTPA is characterized by an unacceptably high *in vivo* lability despite of its excellent thermodynamic stability,[10] which may result in haematopoetic toxicity due to bone marrow irradiation, while ^{90}Y-DOTA is both kinetically and thermodynamically stable and, for that reason, the basis of applied radiopharmaceuticals like e.g. ^{90}Y-DOTATOC, an analogue modified by [Tyr^3]-octreotide (Figure 1) and used for treatment of neuroendocrine tumors.[11–14] Prior to clinical applications, ^{90}Y-DOTATOC has been extensively studied in terms of labelling, *in vitro* receptor binding and tissue distribution in both human and in rat studies.[11,12,14] Quantitative information on kinetic properties of radiopharmaceuticals at physiological pH is, however, scarce and difficult to obtain, especially in view of the low metal concentrations (10^{-8}–10^{-6} M) present in typical radiopharmaceutical compositions.[1]

The free-ion selective radiotracer extraction (FISRE) is a technique developed to assess the dissociation kinetics and speciation of metal complexes applying Chelex metal/radiotracer extractions from carefully equilibrated complex mixtures

[a]*Department Chemie, Lehrstuhl für Radiochemie, Technische Universität München, Walther-Meissner-Str. 3, 85748 Garching, Germany*

[b]*Klinik und Poliklinik für Nuklearmedizin, Ludwig-Maximilians-Universität München, Marchioninistr. 15, 81377 München, Germany*

[c]*Forschungsneutronenquelle Heinz-Maier-Leibnitz (FRM-II), Technische Universität München, Lichtenbergstr. 1, 85747 Garching, Germany*

**Correspondence to: Denis Jurkin, Department Chemie, Lehrstuhl für Radiochemie, Technische Universität München, Walther-Meissner-Str. 3, 85748 Garching, Germany.*
E-mail: jur@rad.chemie.tu-muenchen.de

Copyright © 2008 John Wiley & Sons, Ltd.

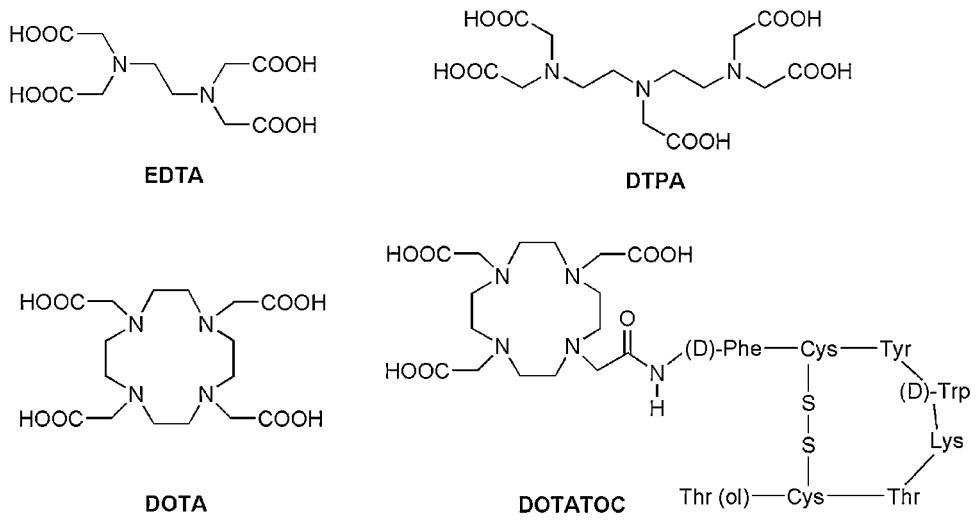

Figure 1. Structural formulas of polyaminocarboxylate ligands.

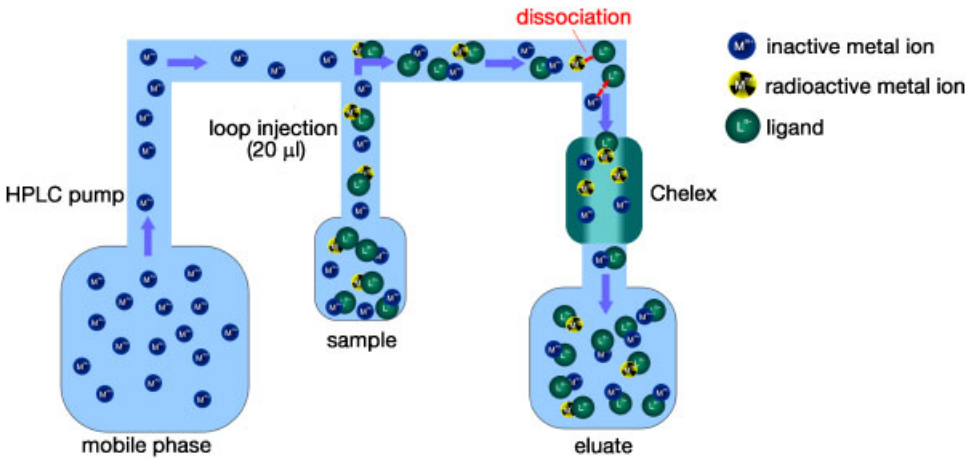

Figure 2. Schematic representation of the FISRE technique.

even at tracer levels. Beside copper and cobalt polyaminocarboxlates, complexes of environmental interest, Ho-DTPA, Ho-DTPA-bispropylamide, Lu-DOTA and Lu-DOTA-[Tyr^3]-octreotate were studied by FISRE.[15–18] Recently, the dissociation kinetics of ^{90}Y-DOTA were analyzed by a modified FISRE method extending the detection limit to be primarily dependent of the half-life of the applied radiotracer and thus allowing the determination of dissociation of inert species.[19] Complementing the latter study, the focus of this work is laid on the analysis of the kinetic stability of ^{90}Y-EDTA, ^{90}Y-DTPA and ^{90}Y-DOTATOC.

First FISRE studies on copper complexes indicated that the presence of free ligand ions potentially disturbs the quantitative adsorption of the metal species due to re-association phenomena.[16] Thus, in addition to the kinetic analysis of the yttrium chelates, we studied the impact of different metal/ligand ratios on the FISRE experiment.

Figure 2 depicts the principle of the FISRE technique. In general, FISRE involves the charge-dependent extraction of free ions. An HPLC pump delivers mobile phase consisting of a buffered aqueous solution of free non-radioactive metal ions to the cation exchange column. A sample containing a carefully equilibrated mixture of ligand, non-radioactive metal ions (in molar excess in relation to the ligand in order to prevent significant amounts of free chelator ions) and the corresponding radiotracer is introduced into the system *via* loop injection. While flowing through the Chelex column metal complexes dissociate with the free metal ion being bound onto the cation exchanger. Provided that the radiotracer is present in the metal complex form quantitatively prior to the injection of the sample, the relative amount of adsorbed radiotracer equals the fraction of dissociated metal complex.

If a (pseudo-) first-order metal complex ($(ML)^{m+n}$) formation equilibrium is considered, where M^m represents the metal ion with charge m, L^n the ligand with charge n Equation (1),

$$M^m + L^n \underset{K_D}{\overset{K_A}{\rightleftharpoons}} (ML)^{m+n} \quad (1)$$

the net dissociation rate can be expressed by the term

$$-\frac{d[(ML)^{m+n}]}{dt} = k_D[(ML)^{m+n}] - k_A[M^m][L^n] \quad (2)$$

The dissociation rate constant k_D (s^{-1}) and the (physico-chemical) complex activity $[(ML)^{m+n}]$ determine the ability of a complex to remain intact within an experimental time scale

Copyright © 2008 John Wiley & Sons, Ltd.

(considering relative values only, physicochemical activity, concentration and radioactivity can be considered equal). Since FISRE uses non-radioactive metal ions in molar excess relatively to the radiotracer and thus a re-association of radiotracer and ligand is statistically disfavored, the association term of Equation (2) can be neglected, resulting in a first-order exponential function as solution

$$[(ML)^{m+n}]_t = [(ML)^{m+n}]_0 \cdot e^{-k_D t} \quad (3)$$

with t being the contact time of the complex with the extracting agent, $[(ML)^{m+n}]_0$ the initial and $[(ML)^{m+n}]_t$ the complex activity at a given contact time. The dissociation rate constant can be determined by plotting the relative activity present in the eluent $[(ML)^{m+n}]_t/[(ML)^{m+n}]_0$ against the contact time t. If two or more kinetically distinguishable complex species are present dissociating independently from each other, the function has to be augmented with i terms that account for the contribution of i species to the detected dissociation profile:

$$[(ML)^{m+n}]_t = \sum_i [(ML)_i^{m+n}]_0 \cdot e^{k_{D_i} t} \quad (4)$$

Consecutive dissociation reactions of two complex species with a rate determining step are given as

$$(ML)_A^{m+n} \overset{k_{D(A)}}{\rightarrow} (ML)_B^{m+n} \overset{k_{D(B)}}{\rightarrow} M^m + L^n \quad (5)$$

requires an additional term that accounts for the formation of $(ML)_B^{m+n}$ from $(ML)_A^{m+n}$:

$$[(ML)^{m+n}]_t = [(ML)_A^{m+n}]_0 \cdot e^{-k_{D(A)} t} + [(ML)_B^{m+n}]_0 \cdot e^{-k_{D(B)} t} + \frac{k_{D(A)} \cdot [(ML)_A^{m+n}]_0}{k_{D(B)} - k_{D(A)}} \cdot (e^{-k_{D(A)} t} - e^{-k_{D(B)} t}) \quad (6)$$

The resulting dissociation curves can be fitted and analyzed by iterative deconvolution methods to assess the rate constants and initial concentrations of species detected. Since the kinetic constants obtained by FISRE are possibly of a pseudo-first-order nature, they are treated as observed rate constants k_{obs} prior to the assignment to a certain species.

Depending on the acquisition time frame, FISRE may be employed in two different modes. The continuous FISRE mode is based on varying the contact time (0.6–60 s) of metal complex and extracting agent by adjusting the sample flow rate through the column and thus allows short-term dissociation studies. The batch mode is especially suitable for studies on kinetically inert species and requires a different sample preparation. Here, the ligand is equilibrated with the radiotracer first, then non-radioactive metal ions are added followed by Chelex extractions at different time intervals after addition of non-radioactive metal ions at a constant mobile phase flow rate. Provided that equal concentrations of metal, ligand, NaCl and buffer are employed, both FISRE modes can be adjusted to complement each other.

Materials and methods

Materials

All chemicals were of analytical reagent grade. Millipore (MQ) water (Millipore, Schwalbach, Germany) was used for solution preparation. Yttrium(III)-chloride hexahydrate (99.99%), EDTA (ethylenediaminetetraacetic acid, 99.995%), DTPA (diethyleneaminepentaacetic acid, ⩾99%), MES (β-morpholino-ethanesulfonic acid monohydrate), HEPES (4-(2-Hydroxyethyl)piperazine-1-ethane-sulfonic acid, ⩾99.5%), Piperazine (⩾99%), 1-Methylpiperazine (⩾99.5%), nitric acid (65%), hydrochloric acid (37%) and sulphuric acid (96%) were purchased from Sigma-Aldrich (Munich, Germany). DOTA (1,4,7,10-tetraazacyclododecane-1,4,7,10-tetraacetic acid), sodium chloride and sodium hydroxide were obtained from Fluka Chemie (Buchs, Switzerland). Ion extracting agents Chelex-100 (200–400 mesh) and Dowex 50 WX 8 as well as the Poly-Prep columns were purchased from BioRad Laboratories (Munich, Germany). Instant thin layer chromatography (ITLC) silica gel strips were obtained from Pall (Dreieich, Germany). DOTATOC (DOTA-[Tyr^3]-octreotide, ⩾99% determined by LC-MS) was provided by the Klinik und Poliklinik für Nuklearmedizin, Ludwig-Maximilians-Universität München and synthesized by common procedures.[19] No-carrier added $^{90}Y^{3+}$ was obtained from a $^{90}Sr/^{90}Y$-generator. Details of the purification and transformation into the chloride form have been outlined previously.[20] ITLC tests according to previously described procedures in 0.1 M $NaHCO_3$ solution resulted in radiochemical purities higher than 96% for each radiotracer sample.[21]

Sample preparation

In order to avoid precipitates in the mobile phase and the samples under study the thermodynamic equilibrium yttrium speciation was calculated using the software CHEAQSPro prior to solution preparation.[22] Thermodynamic equilibrium constants not present in the database were adopted from NIST database 46.[23]

Stock solutions were prepared by dissolving NaCl and buffer (MES, HEPES, Piperazine) in Millipore water. The pH was adjusted by a 10 M NaOH solution to either 5.0 (Piperazine), 6.0 (MES), 7.0 or 7.4 (HEPES). The mobile phase was prepared by dissolving yttrium(III)-chloride in stock solution ($c(Y^{3+}) = 1 \times 10^{-6}$ mol L^{-1}), the ligand solution by dissolving the corresponding ligands in stock solution. The pH of the solutions was checked regularly. The final samples were prepared by mixing ligand solution, mobile phase and stock solution and spiking the mixture with $^{90}YCl_3$. The final total concentrations of yttrium, ligand and buffer were 1×10^{-6}, 7.5×10^{-7} and 5×10^{-3} mol L^{-1}. Each sample was heated mildly at 60°C for 18 h and equilibrated at least 2 h at room temperature prior to the start of the measurements in order to assure thermodynamic equilibrium. The preparation of yttrium-saturated Chelex-100 columns was described previously.[20] The solvent pathway of Class-LC10A*i* HPLC pump (Shimadzu Corporation, Kyoto, Japan) used for solvent delivery as well as the system parts (pump heads, tubing, injection valve, etc.) were mainly constructed of inert materials (PEEK, Tefzel). Additional PEEK tubing and loop material were purchased from Alltech Grom GmbH (Rottenburg-Hailfingen, Germany). In order to allow the column to equilibrate, Chelex was rinsed with the corresponding mobile phase at a constant flow rate of 0.1 mL min^{-1} for 1 h prior to the actual experiments. Although the analysis of the short-term dissociation reactions by continuous FISRE required an equilibration of the radiotracer with all yttrium species present in the sample and subsequent extractions at different flow rates, in batch FISRE mode the radiotracer was equilibrated with the ligand solution and the extractions were performed at different time intervals after Y^{3+}-addition at a constant flow rate of 1 mL min^{-1}. The effect of different metal/ligand ratios was studied by performing continuous FISRE extractions on samples with constant ligand and buffer concentrations of 7.5×10^{-7} and 5×10^{-3} mol L^{-1}, but Y^{3+}-concentrations varying between

Copyright © 2008 John Wiley & Sons, Ltd.

4×10^{-6} and 1.68×10^{-5} mol L^{-1}. Generally, for each extraction 20 μL sample was introduced into the system *via* loop injection. Eluents with a total volume of 1 mL were collected.

A PerkinElmer Tri-Carb 2800 TR LSC-counter was employed to measure the Čerenkov radiation caused by high-energy β-particles emitted by ^{90}Y. The extraction procedures were conducted three times for reproducibility purposes; total Čerenkov radiation per sample was determined by carrying out measurements in absence of the column. All measurements were performed at room temperature (20°C).

Data processing

The concentration of recovered yttrium species was derived by the ratio of the sample Čerenkov radiation to the total Čerenkov radiation measured within each 20 μL aliquot introduced to the system. Plots of recovered yttrium concentration against either contact time with the extracting agent or time elapsed after addition of non-radioactive yttrium solution were used for data analysis. Initially, iterative deconvolution methods based on non-linear regression analysis were applied to assess the number of kinetically distinguishable species.[24–26] Corresponding rate constants k_{obs} and initial concentrations of yttrium species were determined by the fit functions (Equations (3), (4) and (6)) generated with the curve fitting software LABFit.[27]

Results and discussion

Yttrium-EDTA

The short- and long-term dissociation patterns of Y-EDTA are depicted in Figures 3 and 4. A single species fit according to Equation (3) is in good agreement ($R^2_{YY}(x)$0.998) with the dissociation pattern indicating the highly pH dependent dissociation of one species. At pH 5.0, the complex is already completely dissociated after 40 s Chelex contact time, whereas at pH 7.4 the complex requires 8 h to quantitatively exchange the yttrium ions. Below pH 7, dissociation of Y(EDTA)$^-$ is known to occur predominantly *via* proton-assisted pathways. Indeed, the double-logarithmic plot of k_{obs} against the proton concentration as depicted in Figure 10 reveals a linear dependence consistent with a pseudo first-order rate constant being

$$k_{obs} = k_{D0} + k_{D1}[H^+] \quad (7)$$

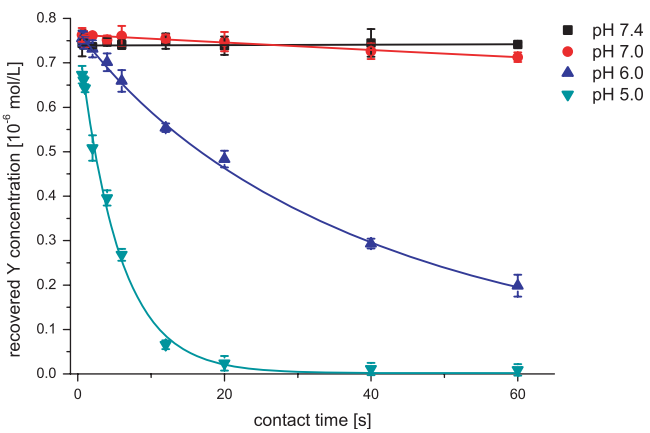

Figure 3. Dissociation profiles of Y-EDTA as detected by the continuous FISRE experiment in dependence of pH with the corresponding first-order curve fit functions ($I = 0.01$, $N = 3$).

Although ^{1}H-NMR studies by Laurenczy *et al.* indicate a spontaneous dissociation rate of the non-protonated species k_{D0} of 1×10^{-4} s^{-1}, which is close to the value calculated in our study

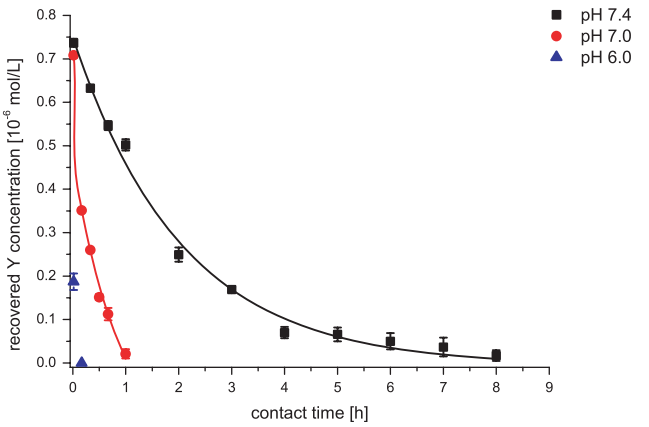

Figure 4. Dissociation profiles of Y-EDTA as detected by the batch FISRE experiment in dependence of pH with the corresponding curve fit functions ($I = 0.01$, $N = 3$).

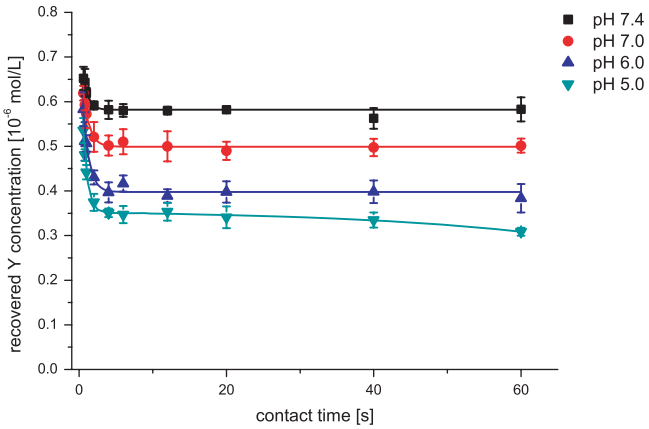

Figure 5. Dissociation profiles of Y-DTPA as detected by the continuous FISRE experiment in dependence of pH with the corresponding second-order curve fit functions ($I = 0.01$, $N = 3$).

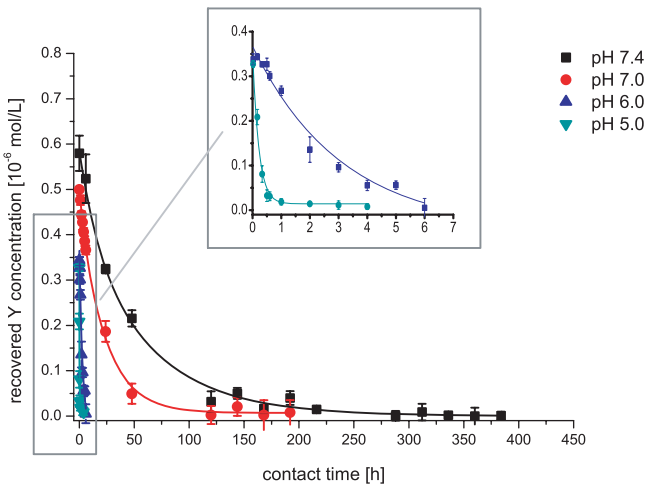

Figure 6. Dissociation profiles of Y-DTPA as detected by the batch FISRE experiment in dependence of pH with the corresponding curve fit functions ($I = 0.01$, $N = 3$).

Copyright © 2008 John Wiley & Sons, Ltd.

Table 1. Kinetic parameters determined by the continuous FISRE mode at different pH values ($I = 0.01$, $N = 3$)

Complex	pH	$c_{Y\text{-}L(A)}$ (10^{-7} mol L^{-1})	$c_{Y\text{-}L(A)}$ (%)	$k_{obs(A)}$ (s^{-1})	$c_{Y\text{-}L(B)}$ (10^{-7} mol L^{-1})	$c_{Y\text{-}L(B)}$ (%)	$k_{obs(B)}$ (s^{-1})
Y-EDTA	7.4	–	–	–	7.44 ± 0.02	99 ± 0.3	$< 3\times10^{-5} \pm 10\times10^{-5}$*
	7.0	–	–	–	7.61 ± 0.02	102 ± 0.3	$< 1.1\times10^{-3} \pm 0.1\times10^{-3}$*
	6.0	–	–	–	7.64 ± 0.05	102 ± 1	$2.35\times10^{-2} \pm 0.06\times10^{-2}$
	5.0	–	–	–	7.56 ± 0.13	100 ± 2	$1.76\times10^{-1} \pm 0.08\times10^{-1}$
Y-DTPA	7.4	1.63 ± 0.44	22 ± 6	1.3 ± 0.4	5.80 ± 0.04	77 ± 1	$< 1\times10^{-4} \pm 3\times10^{-4}$*
	7.0	2.51 ± 0.32	34 ± 4	1.3 ± 0.2	5.01 ± 0.03	67 ± 0.4	$< 1\times10^{-4} \pm 2\times10^{-4}$*
	6.0	4.21 ± 0.98	56 ± 13	1.5 ± 0.3	4.05 ± 0.08	54 ± 1	$< 8\times10^{-4} \pm 7\times10^{-4}$*
	5.0	5.15 ± 0.55	69 ± 7	1.8 ± 0.2	3.57 ± 0.03	48 ± 0.4	$< 2\times10^{-3} \pm 3\times10^{-3}$*
Y-DOTA-TOC	7.4	–	–	–	7.51 ± 0.003	100.1 ± 0.04	$< 6\times10^{-6} \pm 13\times10^{-6}$*
	7.0	–	–	–	7.63 ± 0.004	101.7 ± 0.05	$< 8\times10^{-5} \pm 5\times10^{-5}$*
	6.0	1.47 ± 0.52	20 ± 7	$7.2\times10^{-2} \pm 3.3\times10^{-2}$	6.11 ± 0.54	82 ± 7	$< 9\times10^{-4} \pm 2\times10^{-4}$*
	5.0	2.50 ± 0.22	33 ± 3	$9.8\times10^{-2} \pm 1.4\times10^{-2}$	5.15 ± 0.24	69 ± 3	$< 6\times10^{-4} \pm 9\times10^{-4}$*

The errors represent the standard deviations (S. D.) of three measurements. The kinetic constants marked with asterisks are not justified since the overall uncertainties of the analytical method exceed the S. D. These had to be determined via batch FISRE (Table 2).

(Table 3), the proton-assisted dissociation rate constant of YH(EDTA) k_{D1} exceeds the literature data by orders of magnitude.[28,29] For instance, isotopic exchange reactions studied by Glenthworth *et al.* give k_{D1} values of $30 \pm 1.5\ M^{-1}\ s^{-1}$.[29] Different methodological approaches and experimental conditions may partly contribute to this discrepancy; nevertheless, a detailed explanation is still to be found since common experimental error sources could be ruled out. No pH changes were detected, thus, deviations caused by disturbances in the FISRE experiment due to the formation of double protonated $[YH_2(EDTA)]^+$ in the course of the dissociation are not likely. The fact that Chelex-metal binding becomes less efficient at low pH could implicit higher dissociaton rates as well, but no reduction in yttrium sorption has been observed in the pH range 4.5–7.4 either.

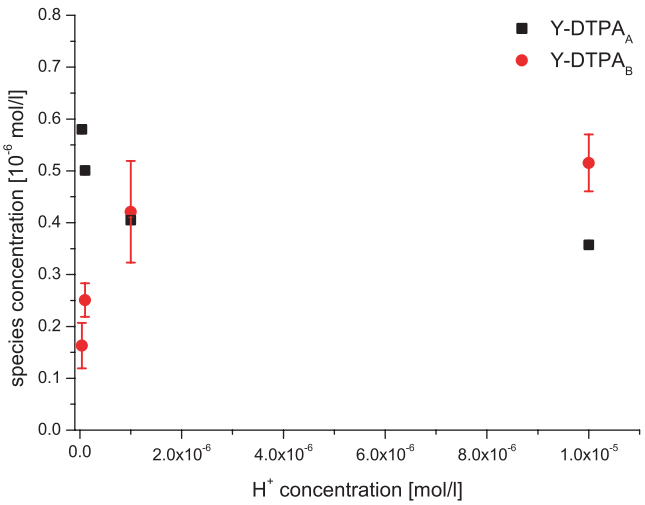

Figure 7. Acid-dependent speciation of Y-DTPA$_A$ and Y-DTPA$_B$ determined by continuous FISRE ($N = 3$).

Y-DTPA

Phenomenologically similar to Y-DOTA,[20] two kinetically distinguishable species are detected during the dissociation of Y-DTPA ($(R^2_{YY}(x)0.996)$). Since the numeric differences are marginal, the pattern can be interpreted in terms of two species dissociating independently from each other (Equation (4)) or a consecutive reaction with the relatively inert species Y-DTPA$_B$ being formed by a labile precursor Y-DTPA$_A$ (Equations (5) and (6)). The labile component Y-DTPA$_A$ cannot be assigned unambiguously and could, for instance, represent an additional species originating from complex isomerism (Figures 5 and 6). The speciation data obtained by continuous FISRE (Table 1) indicate an increase in the Y-DTPA$_A$:Y-DTPA$_B$ ratio with higher proton concentrations (Figure 7) and suggest a saturation behavior similar to the earlier studied Y-DOTA. Although no significant pH-dependence of $k_{obs(A)}$ is observed (Table 1), the kinetically stable species dissociates with a pseudo first-order rate constant according to Equation (7). Besides of a direct attack of endogeneous metal ions, lanthanide-DTPA complexes are, under physiological conditions, considered to predominantly dissociate through proton-assisted processes.[30] The proton-assisted dissociation – characterized by a k_{D1} of $111 \pm 9\ M^{-1}\ s^{-1}$ – exceeds the contribution of the spontaneous dissociation in the considered pH range and corresponds well to an acid-catalyzed k_D of $144\ M^{-1}$ s previously determined by stopped-flow spectrophotometry (0.2 M $NaClO_4$; 25°C).[30,31]

Y-DOTATOC

The short- and long-term dissociation progress of the radiotherapeutic complex depicted in Figures 8 and 9 indicate that, at physiological pH 7.4, no measurable amounts of free $^{90}Y^{3+}$ are released within 27 days. In the same time frame, less than 5% of the total complex dissociate at pH 7.0. A further increase in the proton concentration leads to significantly higher dissociation rates originating from two kinetically distinguishable species each at pH 6.0 and 5.0 (Table 2). The total concentration of the

Copyright © 2008 John Wiley & Sons, Ltd.

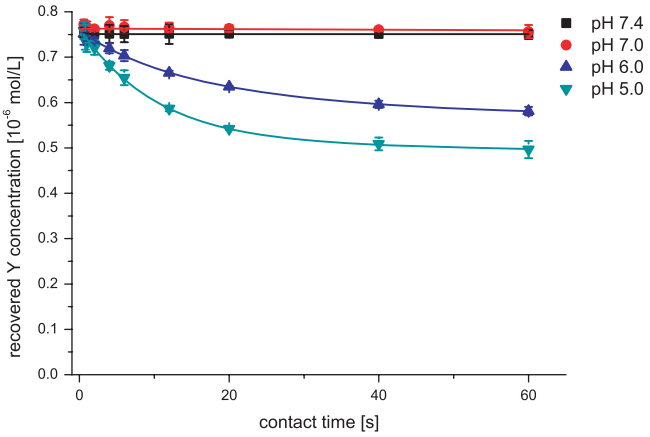

Figure 8. Dissociation profiles of Y-DOTATOC as detected by the continuous FISRE experiment in dependence of pH with the corresponding curve fit functions ($I = 0.01$, $N = 3$).

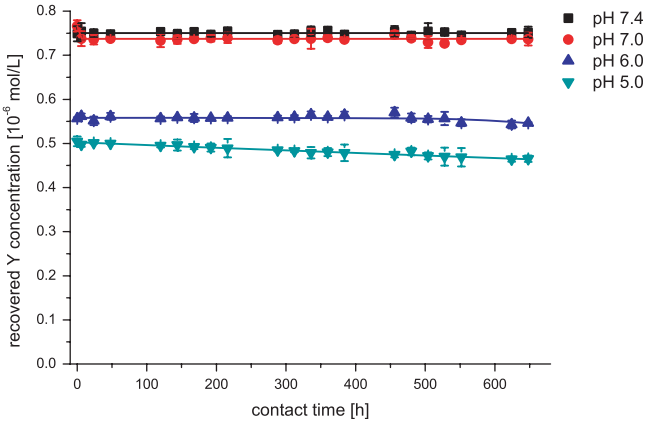

Figure 9. Dissociation profiles of Y-DOTATOC as detected by the batch FISRE experiment in dependence of pH with the corresponding curve fit functions ($I = 0.01$, $N = 3$).

relatively labile species increases with lower pH. The presence of two Y-DOTATOC species suggests that two *cis-*/*trans*-conformation isomers are involved in the dissociation process. Deshmukh *et al.* identified these conformers in aqueous solution at pH 6 by 2D-NMR in the quantitative ratio 67:33, which is basically in agreement with the speciation results listed in Table 1.[32] The kinetic constants $k_{obs(B)}$ obtained by the batch FISRE experiment indicate a linear correlation with the proton concentration according to Equation (7) (Figure 10).

Effects of metal/ligand ratio on FISRE experiments

The assumption that once a metal complex dissociates, the free metal ion is immediately retarded on the Chelex column was examined by performing continuous FISRE measurements at constant pH 6.0 and different yttrium/ligand ratios with EDTA, DTPA, DOTA and DOTATOC. Figure 11 depicts the dissociated fraction of yttrium species after 60 s Chelex contact time in dependence of the metal/ligand ratios. In case of the complexes of acyclic ligands EDTA and DTPA, constant dissociation and speciation are observed until a sharp decline at a metal/ligand ratio of 1. The decline detected with complexes Y-DOTA and Y-DOTATOC is moderate, but already setting in at a metal/ligand ratio of approximately 0.8. Assumably, the cyclic ligand framework of DOTA is able to partly shield the extracting agent off from free yttrium ions even under surplus of metal ions. The fact that the measured dissociation decreases despite of the introduction of additional yttrium ions *via* the mobile phase ($c(Y^{3+}) = 1 \times 10^{-6}\,mol\,L^{-1}$) leads to the conclusion that the mixing of mobile phase and sample is incomplete at the given experimental conditions and the initial sample composition is decisive for the unidirectional dissociation progress. In general, it is evident that the presence of free ligand ions interfere with Chelex FISRE experiments and may potentially result in dissociation rates lower than they actually are. The metal/ligand ratio of 0.75 applied for all kinetic measurements presented here was shown to be appropriate, however (Table 3).

Table 2. Kinetic parameters determined by the batch FISRE mode at different pH values ($I = 0.01$, $N = 3$)

Complex	pH	$c_{Y\text{-}L(A)}$ (10^{-7} mol L^{-1})	$c_{Y\text{-}L(A)}$ (%)	$k_{obs(B)}$ (s^{-1})
Y-EDTA	7.4	7.56 ± 0.02	100.8 ± 0.3	$1.39\times10^{-4} \pm 0.07\times10^{-4}$
	7.0	7.21 ± 0.04	96.1 ± 0.5	$9.2\times10^{-4} \pm 0.1\times10^{-4}$
	6.0	–	–	–
	5.0	–	–	–
Y-DTPA	7.4	5.80 ± 0.01	77.3 ± 0.1	$5.9\times10^{-6} \pm 0.3\times10^{-6}$
	7.0	4.90 ± 0.05	65.3 ± 0.7	$1.2\times10^{-5} \pm 0.1\times10^{-5}$
	6.0	3.74 ± 0.12	50 ± 2	$1.2\times10^{-4} \pm 0.1\times10^{-4}$
	5.0	3.58 ± 0.17	48 ± 2	$1.1\times10^{-3} \pm 0.1\times 10^{-3}$
Y-DOTATOC	7.4	7.50 ± 0.01	100.0 ± 0.1	$<5\times10^{-10} \pm 13\times10^{-10}$*
	7.0	7.37 ± 0.02	98.3 ± 0.3	$<8\times10^{-10} \pm 19\times10^{-10}$*
	6.0	5.61 ± 0.02	74.8 ± 0.3	$5.3\times10^{-9} \pm 0.3\times10^{-9}$
	5.0	5.02 ± 0.01	66.9 ± 0.1	$3.3\times10^{-8} \pm 0.2\times10^{-8}$

The errors represent the S. D. of three measurements. In case of Y-DOTATOC, the kinetic constants determined at pH 7.0 and 7.4 fall below the detection limit of batch FISRE with the overall uncertainties of the analytical method exceeding the S. D.(*).

Copyright © 2008 John Wiley & Sons, Ltd.

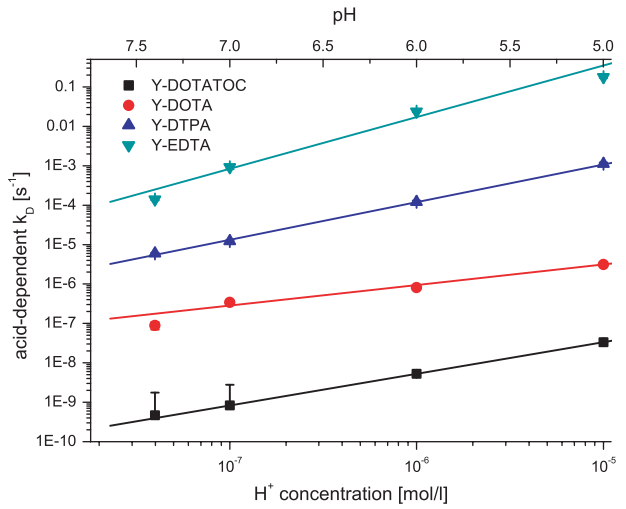

Figure 10. Double logarithmic plot of the proton-assisted dissociation rate constants of Y-EDTA, YDTPA, Y-DOTA[20] and Y-DOTATOC in dependence of proton concentration/pH ($I = 0.01$, $N = 3$) and the corresponding linear fits.

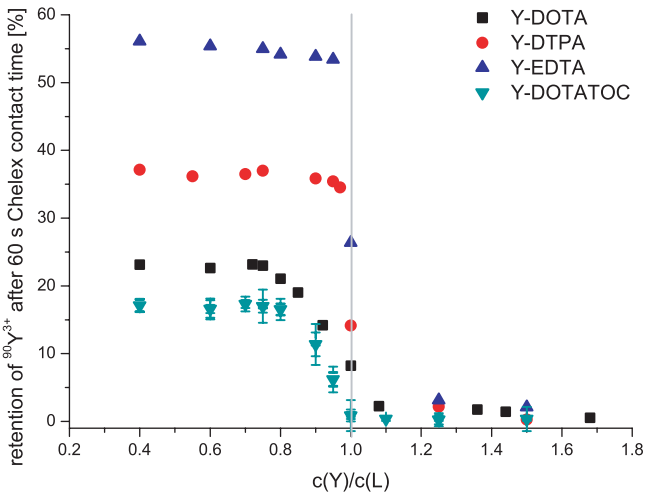

Figure 11. Dissociated fractions of yttrium complexes in dependence of the metal/ligand ratios after 60 s contact time with Chelex (pH = 6.0, $I = 0.01$, $N = 3$).

Table 3. Rate constants for the spontaneous dissociation of non-protonated species (k_{D0}) and acid-dependent dissociation of the single protonated complex species (k_{D1})

Complex	k_{D0} (s^{-1})	k_{D1} ($M^{-1}s^{-1}$)
Y-EDTA	$1.4\times10^{-3}\pm0.1\times10^{-3}$	$1.76\times10^{4}\pm0.80\times10^{4}$
Y-DTPA	$3.8\times10^{-6}\pm0.2\times10^{-6}$	111 ± 9
Y-DOTA[20]	$7.4\times10^{-8}\pm0.2\times10^{-8}$	$2.5\times10^{-2}\pm0.1\times10^{-2}$
Y-DOTATOC	$9\times10^{-10}\pm6\times10^{-10}$	$3.3\times10^{-3}\pm2\times10^{-5}$

Comparison between the dissociation kinetics of Y-EDTA, Y-DTPA, Y-DOTA and Y-DOTATOC

Except for Y-EDTA, within a time frame of 0.6 s–648 h two species were detected to contribute to the dissociation patterns of considered yttrium polyaminocarboxylates. As expected, the acid-dependent rate constants confirm that kinetic lability of the complexes decreases with higher ligand denticity from the hexadentate EDTA to the octadentate DTPA. Compared to the open-chain ligands, the cyclic octadentate DOTA forms a kinetically inert yttrium complex. A significant kinetic stability gain is achieved upon peptide coupling. The kinetic stability order Y-DOTA > Y-DTPA > Y-EDTA (Figure 10) is in accordance with the thermodynamic equilibrium constant order ($K_{Y\text{-}DOTA} = 24.0$, $K_{Y\text{-}DTPA} = 22.05$, $K_{Y\text{-}EDTA} = 18.08$ (25°C, $I = 0.1$)).[33–35]

Conclusions

Dissociation rate constants and time-dependent speciation of yttrium polyaminocarboxylates were sucessfully determined. FISRE proved to be a suitable technique to experimentally determine kinetic data within high acquisition time frames if a good control of interacting parameters is upheld and the results are interpreted carefully. Low costs in equipment and maintenance could make FISRE attractive for the use in pre-clinical *in vitro* kinetic stability screenings and allow complementation with numerical data, especially in the view of fast growing numbers of nuclide (e.g. ^{68}Ga, ^{177}Lu, ^{111}In) and ligand (DOTATATE, DOTANOC, etc.) combinations used in nuclear medicine. For sophisticated solution compositions, additional FISRE improvements are desirable. For instance, charge-dependent kinetics analysis could be enhanced by the application of anion exchangers, while diffusion techniques potentially allow size-dependent speciation. Ideally, the species under study have to interact or be retained quantitatively and selectively; thus, the search for suited exchange material and/or experimental conditions is indispensable for future FISRE developments.

Acknowledgement

The authors thank the Deutsche Forschungsgemeinschaft (DFG) for their financial support under grant WI 3115/1-1, Isotope Technologies Munich AG (ITM AG) for the supply of ^{90}Y and Prof. Dr Andreas Türler for continuing support.

References

[1] S. Liu, *Chem. Soc. Rev.* **2004**, *33*, 445.
[2] S. Liu, D. S. Edwards, *Bioconjugate Chem.* **2001**, *12*, 7.
[3] W. A. Volker, T. J. Hoffman, *Chem. Rev.* **1999**, *99*, 2269.
[4] D. E. Reichert, J. S. Lewis, C. J. Anderson, *Coord. Chem. Rev.* **1999**, *184*, 3.
[5] O. Ugur, L. Kostakoglu, E. T. Hui, D. R. Fisher, K. Garmestani, O. A. Gansow, N. K. V. Cheung, S. M. Larson, *Nucl. Med. Biol.* **1996**, *23*, 1.
[6] G. L. Griffiths, Radiochemistry of therapeutic radionuclides, in *Cancer Therapy With Radiolabeled Antibodies* (Ed.: D. M. Goldenberg), CRC Press, Boca Raton, FL, **1995**, p. 47.
[7] O. A. Gansow, C. Wul, Advanced methods for radiolabeling monoclonal antibodies with therapeutic radionuclides, in *Cancer Therapy with Radiolabeled Antibodies* (Ed.: D. M. Goldenberg), CRC Press, Boca Raton, FL, **1995**, p. 63.
[8] M. Li, C. F. Meares, G. R. Zhong, L. Miers, C. Y. Xiong, S. J. DeNardo, *Bioconjugate Chem.* **1994**, *5*, 101.
[9] M. K. Moi, S. J. DeNardo, C. F. Meares, *Cancer Res. (Suppl.)* **1990**, *50*, 789s.
[10] A. E. Martell, R. M. Smith, *Critical Stability Constants*, Plenum Press, New York, **1974**.
[11] A. Otte, E. Jermann, M. Behe, M. Goetze, H. C. Bucher, H. W. Roser, A. Heppeler, J. Müller-Brand, H. R. Mäcke, *Eur. J. Nucl. Med.* **1997**, *24*(7), 792.

Copyright © 2008 John Wiley & Sons, Ltd.

[12] M. de Jong, W. H. Bakker, E. P. Krenning, W. A. P. Breeman, M. E. van der Pluijm, B. F. Bernard, T. J. Visser, E. Jermann, M. Behe, P. Powell, H. R. Mäcke, *Eur. J. Nucl. Med.* **1997**, *24*(4), 368.
[13] W. A. Breeman, M. de Jong, D. J. Kwekkeboom, *Eur. J. Nucl. Med.* **2001**, *28*, 1421.
[14] R. Valkema, S. A. Pauwels, L. K. Kvols, D. J. Kwekkeboom, F. Jamar, M. de Jong, R. Barone, S. Walrand, P. P. M. Kooij, W. H. Bakker, J. Lasher, E. P. Krenning, *J. Nucl. Med.* **2005**, *46*(1), 83S.
[15] J. van Doornmalen, H. Th. Wolterbeek, J. J. M. de Goeij, *Anal. Chim. Acta* **2002**, *464*, 141.
[16] J. van Doornmalen, *PhD thesis*, Delft University of Technology, **2002**.
[17] B. Wierczinski, A. G. Denkova, J. A. Peters, H. T. H. Wolterbeek, Kinetic stability of metal complexes – determination of k_a and k_d using radiotracers, in *Application of Radiotracers in Chemical, Environmental and Biological Sciences*, *Vol. 1* (Eds.: S. Lahiri, D. Nayak, A. Mukhopadhyay), Saha Institute of Nuclear Physics (Kolkata, India), **2006**, p. 112.
[18] A. G. Denkova, *Diploma thesis*, Delft University of Technology, **2005**.
[19] M. Schottelius, M. Schwaiger, H. J. Wester, *Tetrahedron Lett.* **2003**, *44*(11), 2393.
[20] D. Jurkin, F. J. Gildehaus, B. Wierczinski, *Anal. Chem.* **2007**, *79*(24), 9420.
[21] S. Malja, K. Schomacker, E. Malja, *J. Radioanal. Nucl. Chem.* **2000**, *245*(2), 403.
[22] W. Verweij, *CHEAQSPro*: *A Program for Calculating Chemical Equilibria in Aquatic Systems*, Version 2006.1, RIVM, Bilthoven, **2006**.
[23] A. E. Martell, R. M. Smith, *NIST Critically Selected Stability Constants of Metal Complexes Database*, Version 4.0, NIST Standard Reference Database 46, NIST, Gaithersbourg, MD, **1997**.
[24] A. E. McKinnon, A. G. Szabo, D. R. Miller, *J. Phys. Chem.* **1977**, *81*(16), 1564.
[25] Y. Lu, C. L. Chakrabarti, M. H. Back, D. C. Grégoire, W. H. Schroeder, A. G. Szabo, L. Bramall, *Anal. Chim. Acta* **1994**, *288*, 131.
[26] Y. Lu, C. L. Chakrabarti, M. H. Back, D. C. Grégoire, W. H. Schroeder, *Anal. Chim. Acta* **1994**, *293*, 95.
[27] W. Silva, C. M. D. P. S. Silva, *LAB Fit Curve Fitting Software*: *Nonlinear Regression and Treatment of Data Program*, Version 7.2.33, **2005**.
[28] G. Laurenczy, L. Radics, E. Brücher, *Inorg. Chim. Acta* **1983**, *75*, 219.
[29] P. Glentworth, D. A. Newton, *J. Inorg. Nucl. Chem.* **1971**, *33*, 1701.
[30] E. Brücher, *Top. Curr. Chem.* **2002**, *221*, 103.
[31] T. J. McMurry, C. G. Pippin, C. Wu, K. A. Deal, M. W. Brechbiel, S. Mirzadeh, O. A. Gansow, *J. Med. Chem.* **1998**, *41*, 3546.
[32] M. V. Deshmukh, G. Voll, A. Kühlewein, H. R. Mäcke, J. Schmitt, H. Kessler, G. Gemmecker, *J. Med. Chem.* **2005**, *48*, 1506.
[33] E. Szilágyi, É. Tóth, E. Brücher, A. Merbach, *J. Chem. Soc. Dalton Trans.* **1999**, *15*, 2481.
[34] K. Kumar, C. A. Chang, L. C. Francesconi, D. D. Dischino, M. F. Malley, J. Z. Gougoutas, M. F. Tweedle, *Inorg. Chem.* **1994**, *33*, 3567.
[35] G. Anderegg, *Critical Survey of Stability Constants of EDTA Complexes.* IUPAC Chemical Data Series No. 14, Pergamon, Oxford, **1977**.

Copyright © 2008 John Wiley & Sons, Ltd.